Proc. Natl. Acad. Sci. USA
Vol. 79, pp. 3744–3748, June 1982
Biophysics

Infrared spectroscopy of photodissociated carboxymyoglobin at low temperatures

(Fourier-transform spectroscopy/CO stretching vibration/multiple states/heme pocket/protein relaxation)

J. O. ALBEN[a], D. BEECE[b], S. F. BOWNE[b], W. DOSTER[b], L. EISENSTEIN[b], H. FRAUENFELDER[b,c], D. GOOD[b,d], J. D. MCDONALD[e], M. C. MARDEN[b,f], P. P. MOH[a], L. REINISCH[b], A. H. REYNOLDS[b,g], E. SHYAMSUNDER[b], AND K. T. YUE[b]

[a]Department of Physiological Chemistry, Ohio State University, Columbus, Ohio 43210; and [b]Department of Physics and [e]Department of Chemistry, University of Illinois, Urbana, Illinois 61801.

Contributed by Hans Frauenfelder, March 22, 1982

ABSTRACT **We have studied the infrared spectra of the bound and photodissociated states of Mb-^{12}CO and Mb-^{13}CO from 5.2 to 300 K. The absorbance peaks seen between 1800 and 2200 cm^{-1} correspond to CO stretching vibrations. In the bound state of Mb-^{12}CO, the known lines A_0 at 1969, A_1 at 1945, and A_2 at 1927 cm^{-1}, have center frequencies, widths, and absorbances that are independent of temperature between 5.2 and 160 K. Above 160 K, A_2 gradually shifts to 1933 cm^{-1}. The low-temperature photodissociated state (Mb*) shows three lines (B_0, B_1, B_2) at 2144, 2131, and 2119 cm^{-1} for ^{12}CO. The absorbances of the three lines depend on temperature. B_0 is tentatively assigned to free CO in the heme pocket and B_1 and B_2, to CO weakly bound to the heme or heme pocket wall. The data are consistent with a model in which photodissociation of MbCO leads to B_1 and B_2. B_2 decays thermally to B_1 above 13 K; rebinding to A occurs from B_1. The barriers between B_2 and B_1 and between B_1 and A are described by activation enthalpy spectra. Heme and the central metal atom in state Mb* have near-infrared, EPR, and Mössbauer spectra that differ slightly from those of deoxyMb. The observation of essentially free CO in state B implies that the difference between Mb* and deoxyMb is not due to an interaction of the flashed-off ligand with the protein but is caused by an incomplete relaxation of the protein structure at low temperatures.**

The reversible binding of CO to the storage protein Mb can be studied with flash photolysis (1). Experiments in which the Soret line was monitored demonstrate that the binding process involves a number of steps (2, 3). Here we show that monitoring the CO stretching vibration reveals additional features of the protein's interior.

The active center of Mb, the heme group, is embedded in the protein (Fig. 1) (4) and the ligand binds at the central heme iron. In flash photolysis, the bound-state MbCO is photodissociated. Below 200 K the CO cannot leave the heme pocket and rebinds from there. Two states are involved in low-temperature recombination: state A, in which the CO is bound, the heme is nearly planar, and the iron atom has spin 0; and state B, in which the CO is photodissociated from the heme iron and remains in the protein pocket and the iron has spin 2. At low temperatures, the rebinding process B to A is not exponential in time. We have explained this observation by postulating the existence of conformational substates (2, 5). At low temperatures each Mb molecule is frozen into a particular substate with a specific barrier height for rebinding. From 180 to 80 K the transition occurs by an over-the-barrier Arrhenius process; below 60 K, quantum mechanical tunneling dominates (6, 7). State B (Mb*) has been studied in MbCO and CoMbCO by near-infrared (8, 9), EPR (10, 11), and Mössbauer (12) spectroscopy. These methods are sensitive to the heme group and the metal ion; they indicate that Mb* differs from deoxyMb. Is this difference due to the ligand perturbing the heme after photodissociation or to some other mechanism such as incomplete relaxation of the heme after photolysis at low temperatures? Infrared spectroscopy, which monitors the ligand rather than the heme, helps to answer this question and provides new insight into the behavior of the photodissociated ligand in the pocket.

EXPERIMENTAL

Lyophilized sperm whale Mb from Sigma (St. Louis, MO) or Pentex (Kankakee, IL) was dissolved in 70% (vol/vol) glycerol in water buffered to pH 7 with 0.1 M phosphate. The sample was stirred under a CO atmosphere for several hours, reduced with sodium dithionite, and stirred for several more hours to form MbCO. The final protein concentration was about 15 mM. The sample then was transferred to a sample holder with calcium fluoride or sapphire windows and a path length of 0.1 or 0.2 mm. For temperature measurements, a gold–chromel thermocouple bead was embedded in the sample. Spectra were taken on a Digilab and a Nicolet 7199 Fourier-transform infrared spectrometer at 1- or 2-cm^{-1} resolution. As controls, some samples were dialyzed against glycerol to remove buffer, water, and dithionite and some samples were run with no thermocouple (a thermal diode was used to measure the temperature of the sample holder). Neither dialysis nor the thermocouple bead produced any measurable effect.

Spectra with ^{12}CO and with mixtures of ^{12}CO and ^{13}CO were obtained by cooling the sample in the dark to the desired temperature and taking a bound-state single-beam intensity spectrum $I_A(\nu)$ (Fig. 2). The sample then was illuminated with a tungsten light source. Within a few minutes, equilibrium between photodissociation and rebinding was reached and $I_{eq}(\nu)$ was measured. States A and B both contribute to $I_{eq}(\nu)$. The fraction due to state B depends on light intensity and temperature; for our experimental conditions the fraction was >99% at 20 K, but only 60% at 60 K. Absorbance spectra are computed as $\Delta A(\nu) = \log[I_{eq}(\nu)/I_A(\nu)]$; an example is given in Fig. 3. The total absorbance change under a line is, with complete photo-

The publication costs of this article were defrayed in part by page charge payment. This article must therefore be hereby marked "*advertisement*" in accordance with 18 U. S. C. §1734 solely to indicate this fact.

[c]To whom reprint requests should be addressed.
[d]Present address: Bell Laboratories, Naperville, IL 60540.
[f]Present address: European Molecular Biology Laboratory, D2000 Hamburg 52, Federal Republic of Germany.
[g]Present address: McDonnell–Douglas Astronautics Company, St. Louis, MO 63166.

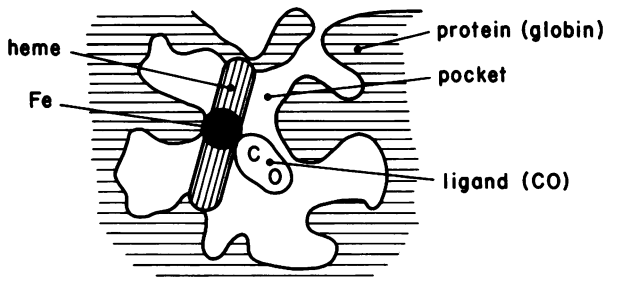

FIG. 1. Schematic cross section through the active center of myoglobin, with CO bound to the heme iron (state A). After photodissociation (state B), the CO remains in the pocket, and the protein does not relax entirely into the deoxy state.

dissociation, given by

$$F \equiv \int_{\text{line}} d\nu\, \Delta A(\nu) = cl \int d\nu\, \varepsilon(\nu). \qquad [1]$$

Here, c is the concentration, l is the path length, and $\varepsilon(\nu)$ the extinction coefficient at wavenumber ν. The protein concentration is determined by comparing our data to previous measurements on MbCO (13).

RESULTS AND INTERPRETATION

We measured the infrared spectra of the bound and photoequilibrated states (MbCO + Mb*) at various temperatures between 5.2 and 100 K. Comparison of the ^{12}CO and ^{13}CO spectra allows us to assign every absorbance peak in Fig. 3 unambiguously to CO, because the $Mb^{12}CO$ and $Mb^{13}CO$ spectra have the same shape, but every line of the heavier isotope is shifted to lower wavenumbers by the expected amount. Fig. 4 gives the absorbance changes between 2050 and 2130 cm^{-1} at two temperatures with an expanded scale. Figs. 2–4 show that three lines appear in the bound state A (A_0 at 1969, A_1 at 1945, and A_2 at 1927 cm^{-1} for ^{12}CO) and three in the photodissociated state B (B_0 at 2144, B_1 at 2131, and B_2 at 2119 cm^{-1} for ^{12}CO). In Table 1 we present center wavenumbers and linewidths of the peaks in MbCO and several standard systems. Line B_0 shows large sample-to-sample variations and we have not been able to correlate its intensity with another observable variable.

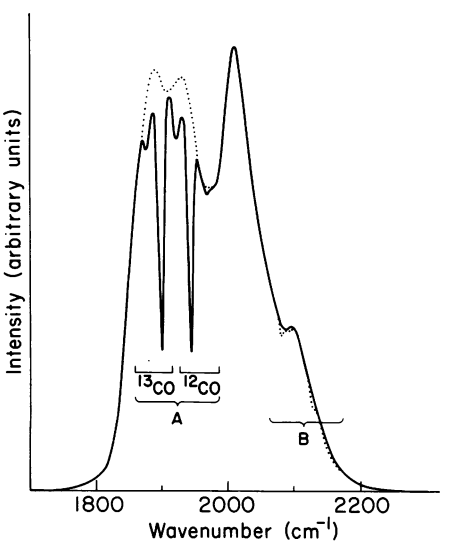

FIG. 2. Intensity spectra of Mb-^{12}CO and Mb-^{13}CO (isotope ratio ≈ 1:1) taken at 14 K on a Digilab FTIR with CaF_2 windows. The solid line represents $I_A(\nu)$, the infrared spectrum taken before illumination. The CO absorption lines in the bound state A are clearly recognizable. The dotted line represents $I_{eq}(\nu)$. At 14 K, >99% of the CO remained in the photodissociated state during illumination and appeared as weak lines around 2100 cm^{-1}.

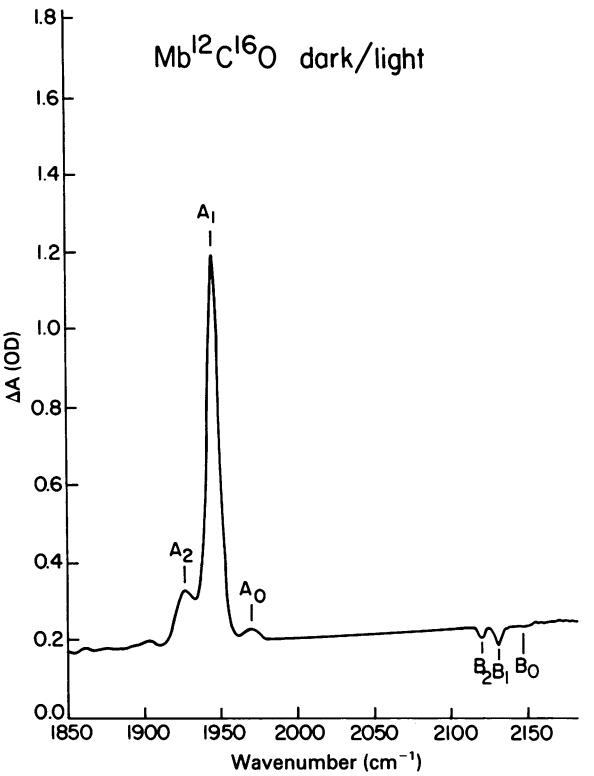

FIG. 3. Absorbance change, $\Delta A(\nu) = \log[I_{eq}(\nu)/I_A(\nu)]$, as a function of wavenumber ν, at 5.5 K, for $^{12}C^{16}O$. The bound states appear around 1900 cm^{-1}; the weak lines of the photodissociated CO are seen around 2100 cm^{-1}.

A complete discussion of the data is not possible at present because we have not yet measured transition rates among the states as function of temperature. Some tentative conclusions, however, can be drawn. The three lines in the covalently bound state A have been interpreted by Makinen *et al.* (17) as corresponding to three different arrangements of the CO, the heme group, and the proximal and distal histidines. Our data are not sensitive to these spatial features but do provide other information. The center wavenumbers of the A_0 and A_1 are independent of temperature between 5.2 and 300 K. A_2 appears at 1927 cm^{-1} between 5.2 and 160 K but shifts gradually toward 1933 cm^{-1} between 160 and 210 K. Above 220 K, the positions of the three lines coincide with the ones observed by Makinen *et al.* (17). A_1, the major band, has a linewidth $\Delta\nu_{1/2}$ of about 8 cm^{-1} that is independent of temperature between 5.2 and 300 K; the line shape is much closer to a Gaussian than a Lorentzian. A_0 and A_2 also have large linewidths that are temperature independent from 5.2 K to at least 210 K. For comparison, solid CO has a linewidth that changes from about 3 cm^{-1} at 30 K to 14 cm^{-1} at 67 K (14, 15). The large, temperature-independent, non-Lorentzian linewidths may be caused by conformational substates (2, 5). In each configuration (A_0, A_1, A_2) the protein may still assume a large number of slightly different isoenergetic structures with somewhat different CO stretching vibrations, leading to a broadened and nearly Gaussian line. The total integrated extinction coefficient for state A is 30.4 ± 0.2 $mM^{-1}cm^{-2}$, considerably larger than the value 2.5 $mM^{-1}cm^{-2}$ for solid CO (15). The large absorbance in state A is caused by the covalent bond between Fe and C which decreases the

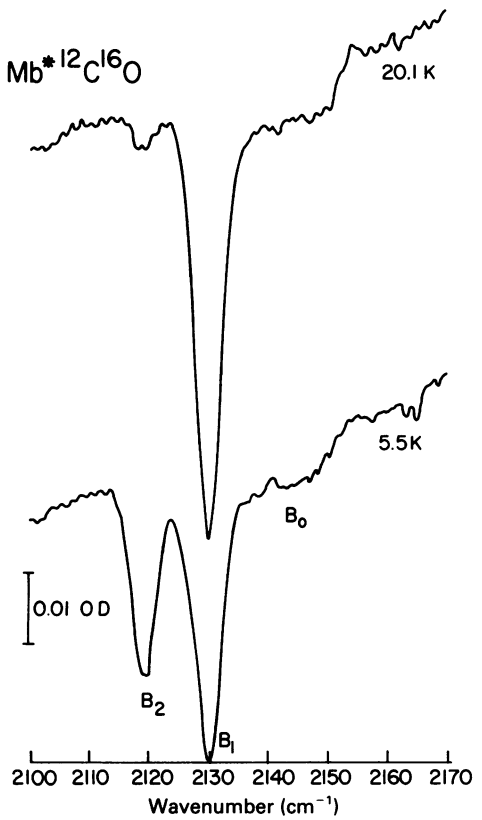

FIG. 4. Absorbance change, $\Delta A(\nu)$, for ^{12}CO in the photodissociated state, Mb*, at 5.5 and 20.1 K. The curves are vertically displaced for clarity. Peak positions appear slightly shifted due to the nonuniform transmission of the glycerol.

strength of the CO bond, increases the CO dipole moment, and shifts the center wavenumber by about 200 cm^{-1} from the free-gas value of 2143 cm^{-1}.

Interpretation of the three lines in the photodissociated state B is more intricate than appears at first. The wavenumber of state B_0 coincides with that of free CO; B_1 is shifted by 12 cm^{-1} and B_2 by 24 cm^{-1} from the free-gas value, 2143 cm^{-1}. In the simplest approximation, the magnitude of the shift in center frequency from the free-gas value will increase with binding enthalpy. The shifts suggest that in B_0 the CO is free within the heme pocket and in B_1 and B_2 it is weakly bound to the heme or the pocket walls. The fact that transitions from B_2 to B_1 and from B_1 to A are observed even at 20 K also suggests weak binding in B.

The integrated extinction coefficient for state B is obtained by noting that the contribution from B_0 is small and constant below 50 K and that rebinding from B to A is very slow below 20 K (7). Below 20 K, we therefore can consider transitions between B_2 and B_1 alone. In Fig. 5 we plot normalized integrated absorption changes, $f_i = F/cl$, for the states B_1 and B_2. Here F is given by Eq. 1 for each state and c is the total Mb concentration. Fig. 5 shows that $f_1 + f_2$ = constant from 5.2 to 20 K: the two lines have equal extinction coefficients, $\varepsilon(B_2)/\varepsilon(B_1) = 1.0 \pm 0.3$. The total integrated extinction coefficient for state B then becomes 1.4 ± 0.1 $mM^{-1}cm^{-2}$. Values of ε smaller than that of the free CO have been observed in other systems (18).

The intricacies of the B states emerge when we consider the temperature dependence of f_1 and f_2 (Fig. 5) in detail. Values of f_1 and f_2 obtained by photodissociation at any temperature between 5.5 and 20 K are shown as open circles in Fig. 5; these values follow the solid lines. If MbCO is photodissociated at 5.5 K and the temperature is then increased, with or without illumination, the resulting values of f_1 and f_2 also follow the solid lines. Up to 13 K, f_1 and f_2 are constant; above 13 K, f_1 increases and f_2 decreases by the same amount. At each temperature, f_1 and f_2 remain constant within errors for at least 10^3 sec. These observations appear to suggest that states B_1 and B_2 are frozen below 13 K and that equilibrium is established above 13 K by transitions from the more tightly bound state B_2 to B_1. This explanation, however, is not tenable because the transition $B_2 \rightarrow B_1$ is not reversible; cooling in the dark from 20 to 4.2 K, indicated by the solid dots and the dashed lines in Fig. 5, leaves

Table 1. Spectral parameters for the CO stretching vibration

System and state	T, K	Line center, cm^{-1}	Linewidth ($\Delta\nu_{1/2}$), cm^{-1}	Ref.
Gas		2143	—	14, 15
Gas†		2096	—	14
Liquid	69	2139	16	14
Solid	59	2139	2	14
Solid†	59	2092	2	14
Solid	30	2138	2.8	15
Argon matrix	6	2138	0.6	16
Mb:A_0	273–300	1967	8 ± 1	17
:A_1	273–300	1944	9 ± 1	17
:A_2	273–300	1933	10 ± 2	17
Mb:A_0	5.5–210	1969 ± 1	8 ± 1	*
:A_1	5.5–210	1944.8 ± 0.5	8 ± 1	*
:A_2	20	1927.0 ± 0.2	17 ± 2	*
:A_0†	20–210	1924 ± 1	8 ± 1	*
:A_1†	20–210	1900.8 ± 0.5	8 ± 1	*
:A_2†	20–210	1885 ± 1	16 ± 2	*
Mb:B_0†	14–100	2099 ± 3	12 ± 4	*
:B_1†	14–100	2083.7 ± 0.5	5.2 ± 0.1	*
:B_2†	14–40	2072.3 ± 0.5	4.2 ± 0.5	*
:B_0	5.5–100	2146 ± 3	12 ± 4	*
:B_1	5.5–100	2130.5 ± 0.5	5 ± 0.5	*
:B_2	5.5–30	2119.0 ± 0.5	4.5 ± 0.5	*

* Data from present work.
† These rows are for $^{13}C^{16}O$; the others refer to $^{12}C^{16}O$.

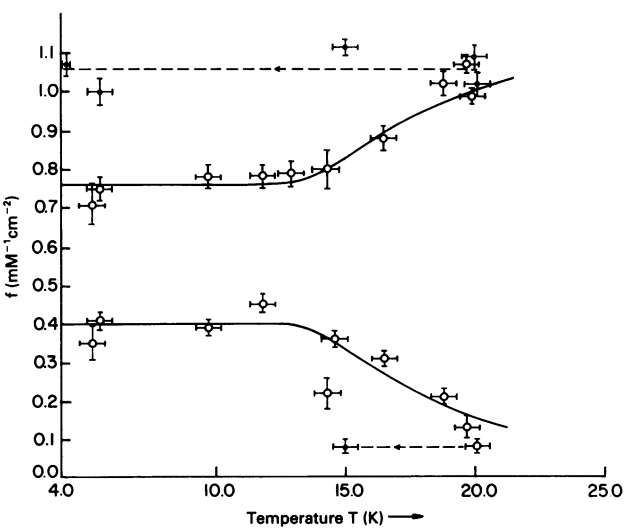

FIG. 5. Plot of normalized absorbance change $f = \int d\nu\, \Delta A(\nu)/cl$ for the states B_1 and B_2 as function of temperature. Here c is the total Mb concentration and l is the path length in the sample. The data points following the solid lines are taken starting at low temperatures. The solid lines are a fit to the data with Eq. 3. The dashed lines indicate values of f_1 and f_2 obtained on decreasing the temperature from 20 K.

f_1 and f_2 unchanged at the values corresponding to 20 K. B_1 and B_2 cannot be in equilibrium.

We have considered various models to explain the irreversibility but have found only one acceptable one. We assume that B_1 is the state with lower Gibbs energy, that a barrier of height H lies between B_2 and B_1, and that the initial photodissociation leads with probabilities b_2 and b_1 to these states. At <13 K the states remain frozen. At higher temperatures, the molecules in B_2 overcome the barrier to B_1. If the Gibbs energy of B_1 is sufficiently lower than that of B_2, the reverse transition will not be observed. This simple model, however, does not explain the apparent time independence at each temperature. Transitions over a barrier of unique height are exponential in time and we should see an exponential approach to equilibrium. A modification of the model fits all data. We postulate that the barrier between B_2 and B_1 is not unique but is given by an activation enthalpy spectrum (2, 19). The transition $B_2 \rightarrow B_1$ then is not exponential in time but is close to a power law. A power law can simulate time independence, as we will prove. If we denote with $g(H)dH$ the probability of having a barrier with activation enthalpy between H and $H + dH$, and if at time $t = 0$ a CO is in state B_2, the probability $P(t,T)$ of still finding the CO in B_2 at time t is given by $P(t,T) = \int_0^\infty dH\ g(H)\ \exp[-k(H)t]$. Here $k(H)$ is the rate coefficient for a barrier of height H. The population of state B_2 at time t and temperature T is proportional to $f_2(t,T)$ so that

$$f_2(t,T) = f_2(0,T)\ P(t,T). \quad [2]$$

In order to show that the model can fit the data, we use the form of $g(H)$ found in our earlier experiments (2): $g(H)$ peaks at a value H_p and tails off exponentially toward high values of H with coefficient α, $g(H) \propto \exp(-\alpha H)$. Equations 1, 2, 15, and 21 of ref. 2 then give

$$P(t,T) = (1 + t/t_0)^{-n}, \quad [3]$$

$$n = \alpha RT, \quad t_0 = n A^{-1} \exp(H_p/RT). \quad [4]$$

$P(t,T)$ is characterized by three parameters, α, H_p, and A. The data are only good enough to determine two, and we select the preexponential $A = 10^{11\pm2}$ sec^{-1}. A data point in Fig. 5 requires measuring time of the order of 10^2 sec. A fit of Eqs. 2, 3, and 4 to the data, with $t = 10^2$ sec and $A = 10^{11\pm2}$ sec^{-1} yields $\alpha = 0.56 \pm 0.1$ mol kJ^{-1} and $H_p = 3.7 \pm 0.5$ kJ mol^{-1}. The fit is shown as solid lines in Fig. 5. The errors in α and H_p come from the uncertainty in A.

The distributed-barrier model and the observed value of α explain why Fourier-transform infrared experiments can fake equilibrium. The minimum time to take a good data point is about 10^2 sec; experiments beyond 10^3 sec become tedious. Eqs. 2–4 give, at 15 K, $P(10^2 \text{ sec}) = 0.81$, $P(10^3 \text{ sec}) = 0.70$ and, at 20 K, $P(10^2 \text{ sec}) = 0.39$, $P(10^3 \text{ sec}) = 0.32$. The experimental uncertainties are such that these values appear to indicate time independence of F_2; at a given temperature, experiments with the Fourier-transform infrared spectrometer will feign equilibrium. With increasing temperature, however, $P(10^2$ sec) decreases and B_1 becomes more populated and simulates a state of higher enthalpy.

The low-temperature infrared studies presented here solve one question but raise a number of new problems. The question solved is the one asked initially: How does Mb* differ from deoxyMb? X-ray, optical, and near-infrared experiments indicate that the heme group and the surrounding protein structure are not identical in Mb* and deoxyMb. After photodissociation, the heme group and the protein consequently will try to relax to the deoxy state. Since CO is either quasi-free in state B_0 or very weakly bound in states B_1 and B_2, it is unlikely that the ligand will affect the heme group strongly or prevent the relaxation. It is more probable that the frozen configuration allows only a partial transition to the deoxy state at temperatures below 160 K. This observation agrees with results obtained by Blumenfeld (20, 21).

The problems raised by the present work can be described in terms of the scheme that fits the low-temperature data:

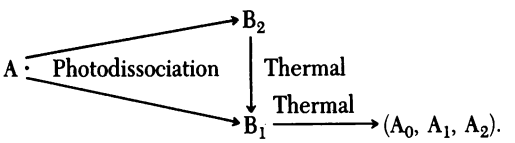

Photodissociation leads from A to B_1 and B_2; thermal transitions lead from B_2 to B_1 and B_1 to A. Both transitions occur over distributed barriers (2). The average barrier height between B_2 and B_1 is of the order of 4 kJ mol^{-1}; between B_1 and A it is 10 kJ mol^{-1}. A great deal of work will be required to explore these states and transitions. To study the time dependence of the transitions $B_2 \rightarrow B_1$ and $B_1 \rightarrow$ A, a fast infrared flash photolysis system will be needed (22). Measurements as function of temperature will show when transitions occur via tunneling (6, 7); they may also indicate if the reaction scheme is as simple as given here or if additional branches occur. The explanation of the various A and B states in terms of the structure of the protein calls for more low-temperature x-ray crystallographic data and for experiments with different proteins.

We thank Mark Ensminger and Mary Moss for their help, William A. Eaton and Marvin W. Makinen for incisive comments, and Richard I. Masel for making experiments with the Nicolet Fourier-transform infrared system possible. This work was supported in part by U.S. Public Health Service Grants GM 18051 and HL 17839, National Science Foundation Grants PCM 79-05072 and 80-17761, and American Heart Association Grant 78-1089. H.F. gratefully acknowledges support from the European Molecular Biology Organisation, S.F.B. had a fellowship from the Minnesota Mining and Manufacturing Company, and W.D. had a fellowship from the Deutsche Forschungsgemeinschaft.

1. Antonini, E. & Brunori, M. (1971) *Hemoglobin and Myoglobin in Their Reactions with Ligands* (North-Holland, Amsterdam).
2. Austin, R. H., Beeson, K. W., Eisenstein, L., Frauenfelder, H. & Gunsalus, I. C. (1975) *Biochemistry* **14**, 5355–5373.
3. Beece, D., Eisenstein, L., Frauenfelder, H., Good, D., Marden, M. C., Reinisch, L., Reynolds, A. H., Sorensen, L. B. & Yue, K. T. (1980) *Biochemistry* **19**, 5147–5157.
4. Norwell, J. C., Nunes, A. C. & Schoenborn, B. P. (1975) *Science* **190**, 568–570.
5. Frauenfelder, H., Petsko, G. & Tsernoglou, D. (1979) *Nature (London)* **280**, 558–563.
6. Alberding, N., Austin, R. H., Beeson, K. W., Chan, S. S., Eisenstein, L., Frauenfelder, H. & Nordlund, T. M. (1972) *Science* **192**, 1002–1004.
7. Alben, J. O., Beece, D., Bowne, S. F., Eisenstein, L., Frauenfelder, H., Good, D., Marden, M. C., Moh, P. P., Reinisch, L., Reynolds, A. H. & Yue, K. T. (1980) *Phys. Rev. Lett.* **44**, 1157–1160.
8. Yonetani, T., Iizuka, T., Yamamoto, H. & Chance, B. (1973) *Oxidases and Related Redox Systems*, eds. King, T. E., Mason, H. S. & Morrison, M. (Univ. Park Press, Baltimore), pp. 401–404.
9. Iizuka, T., Yamamoto, H., Kotani, M. & Yonetani, T. (1974) *Biochim. Biophys. Acta* **371**, 126–139.
10. Yonetani, T., Yamamoto, H. & Iizuka, T. (1973) *J. Biol. Chem.* **249**, 2168–2174.
11. Iizuka, T., Yamamoto, H., Kotani, M. & Yonetani, T. (1974) *Biochim. Biophys. Acta* **351**, 182–195.
12. Spartalian, K., Lang, G. & Yonetani, T. (1976) *Biochim. Biophys. Acta* **428**, 281–290.
13. Yen, L. (1971) Dissertation (Ohio State University, Columbus, OH).

14. Ewing, G. E. (1962) *J. Chem. Phys.* **37,** 2250–2256.
15. Jiang, G. J., Person, W. B. & Brown, K. G. (1975) *J. Chem. Phys.* **62,** 1201–1211.
16. Dubost, H. & Abouaf-Marguin, L. (1972) *Chem. Phys. Lett.* **17,** 269–273.
17. Makinen, M. W., Houtchens, R. A. & Caughey, W. S. (1979) *Proc. Natl. Acad. Sci. USA* **76,** 6042–6046.
18. Brown, T. L. & Darensbourg, D. J. (1967) *Inorg. Chem.* **6,** 971–977.
19. Primak, W. (1955) *Phys. Rev.* **100,** 1677–1689.
20. Blumenfeld, L. A. (1978) *Q. Rev. Biophys.* **11,** 251–308.
21. Blumenfeld, L. A. & Davidov, R. M. (1979) *Biochim. Biophys. Acta* **549,** 255–280.
22. Siebert, F., Mäntele, W. & Kreutz, W. (1980) *Biophys. Struct. Mech.* **6,** 139–146.